Filling in of Fraunhofer and gas-absorption lines in sky spectra as caused by rotational Raman scattering

Christopher E. Sioris and Wayne F. J. Evans

A line-by-line radiative-transfer model to quantify the Ring effect as caused by rotational Raman scattering has been developed for the 310–550-nm spectral interval. The solar zenith angle and the resolution are key input parameters, as is the sky spectrum (excluding inelastic atmospheric scattering), which was modeled with MODTRAN3.5. The filling in is modeled for ground-based viewing geometry and includes surface reflection and single inelastic scattering. It is shown that O_2 contributes half of the filling in of N_2. A strong inverse relationship with wavelength is noted in the filling in. A comparison with observations shows moderate agreement. The largest filling in occurs in the Ca II K and H lines.

OCIS codes: 300.6330, 010.1310, 300.1030.

1. Introduction

The Ring effect was discovered almost 40 years ago when measurements of scattered light were compared with those from direct sunlight.[1] Anomalous Fraunhofer spectra were observed that corresponded to an effective filling in of the Fraunhofer structure.

Many models have been built to simulate filling in (FI), and they provide a comparison with the observed Ring spectra.[2] Brinkmann[3] was the first to attribute FI to rotational Raman scattering (RRS). Kattawar *et al.*[4] stated that the effect due to aerosol fluorescence is too weak to explain observed intensities. They cited published measurements that showed that aerosol fluorescence produces a relevant contribution only when aerosol concentrations occur, which are found, for example, in engine exhausts. They suggested a combination of RRS and Rayleigh–Brouillin scattering (inelastic scattering of photons at sound waves) to explain the Ring effect. The model that they developed to predict the Ring effect showed a strong increase in the FI parameter for an increase in the solar zenith angle because they did not include aerosol scattering. Subsequent models have addressed this shortcoming (e.g., Burrows *et al.*[2]).

Joiner *et al.*[5] used RRS exclusively to model the Ring effect and found good agreement between model values and measurements from the Shuttle Solar Backscatter Ultraviolet Radiometer and the Nimbus-7 Solar Backscatter Ultraviolet Radiometer. Chance and Spurr[6] calculated the Ring effect by using a solar spectrum, thereby ignoring terrestrial absorption. The latest research on modeling the Ring effect[7] uses a novel mathematical approach. Our research also models the Ring effect by using RRS exclusively and examines a wide spectral interval (310–550 nm).

2. Spectroscopic Parameters

Most of the molecules in the atmosphere are in the ground vibrational state ($v = 0$). In this model only the ground vibrational state is considered, and thus the Raman scattering comes purely from rotational transitions in the molecules.

The shifts and the cross sections are the main parameters needed to compute the amount of power from the incident solar beam that is frequency redistributed by RRS. RRS cross sections (square centimeters) are given by

$$Q_{N,J\to N',J'} = 256\pi^5\gamma^2 f_N b_{N,J\to N',J'}/[27(\lambda')^4] \qquad (1)$$

C. E. Sioris is with the Department of Earth and Space Science, York University, 4700 Keele Street, Toronto, Ontario M3J 1P3, Canada. His e-mail address is csioris@yorku.ca. W. F. J. Evans is with the Department of Physics, Trent University, 1600 West Bank Drive, Peterborough, Ontario K9J 7B8, Canada.

Received 5 November 1998; revised manuscript received 25 January 1999.

0003-6935/99/122706-08$15.00/0

(from Chance and Spurr[6]) where γ (cubic centimeters) is the polarizability anisotropy of the species and for oxygen is equal to

$$\gamma_{O_2} = 7.149 \times 10^{-26}\ \mathrm{cm}^3 + 4.59364 \times 10^{-15}\ \mathrm{cm}/(4.82716 \times 10^9\ \mathrm{cm}^{-2} - \nu^2), \quad (2)$$

where ν is the wave number in inverse centimeters. For N_2 the numerically derived dependence on the wave number of the polarizability anisotropy is

$$\gamma_{N_2} = -6.01466 \times 10^{-25}\ \mathrm{cm}^3 + 2.38557 \times 10^{-14}\ \mathrm{cm}/(1.86099 \times 10^{10}\ \mathrm{cm}^{-2} - \nu^2). \quad (3)$$

The Placzek–Teller coefficients are represented by b in Eq. (1); values were obtained from Burrows *et al.*,[2] λ' is the wavelength of the shifted line (in centimeters), J is the total angular momentum quantum number, and N is the nuclear rotational angular momentum quantum number. J and J' represent the initial and the final states, respectively. The same notation is used with N. Note that the total electronic spin angular momentum quantum number (S) represents the difference between J and N.[8] For oxygen $S = 1$, whereas for nitrogen $S = 0$. Thus for nitrogen $N = J$ and Eq. (1) simplifies to

$$Q_{N\to N'} = 256\pi^5\gamma^2 f_N b_{N\to N'}/[27(\lambda')^4]. \quad (4)$$

But for oxygen there are multiple cases that can be described by $N = J, J \pm 1$.

We calculated fractional populations in the initial state by using

$$f_N = (g_N/Z)(2J + 1)\exp(-E/kT), \quad (5)$$

where g_N is the statistical weight factor for the initial state owing to the rotational spin. For nitrogen $g_N = 6$ and $g_N = 3$ for even and odd N, respectively.[5] This factor results in alternating line intensities as shown in Fig. 1(a). For oxygen $g_N = 0$ and $g_N = 1$ for even and odd N, respectively, which explains the absence of even N lines in Fig. 1(b). $E(J)$ is the rotational energy, k (joules/Kelvin) is the Boltzmann constant, and $T(K)$ is the absolute temperature. Rotational energies are approximated by $E = hcB(N + 1)(N)$, where B is the rotational constant, h is Planck's constant, and c is the speed of light. B has a value of 1.9897 cm^{-1} for N_2 and 1.438 cm^{-1} for O_2.[5]

In the case of purely RRS the state sum Z reduces to

$$Z = \sum_{J,N} f_N. \quad (6)$$

Rotational Raman transitions for linear molecules such as O_2 and N_2 have the selection rule: $\Delta N = N' - N = 0, \pm 2$.[7] Stokes transitions have $\Delta N = 2$, whereas transitions with $\Delta N = -2$ are called anti-Stokes. Accurate shifts were again available from Burrows *et al.*[2]

For modeling the RRS the atmosphere was considered to be 80% N_2 and 20% O_2.

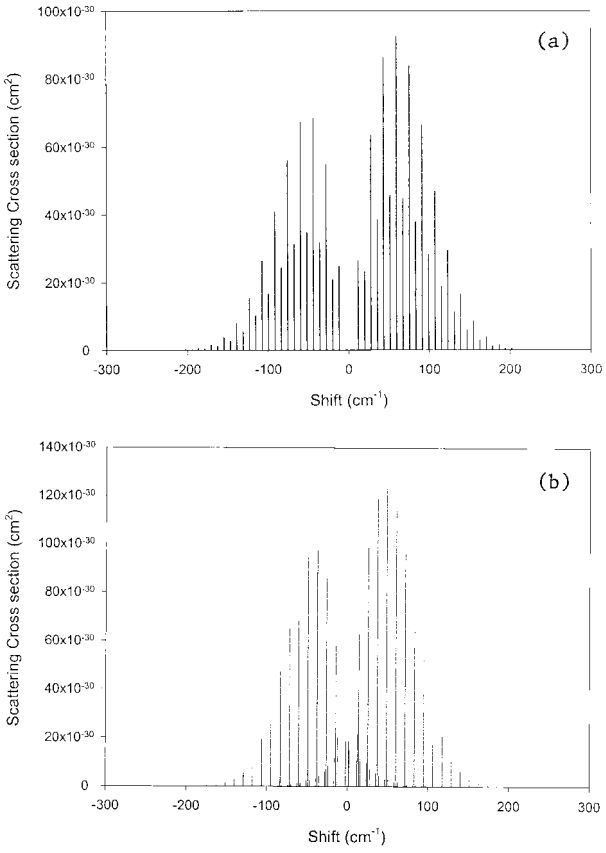

Fig. 1. (a) Rotational Raman spectrum of N_2 at 258 K, 310 nm. Anti-Stokes lines are shifted to shorter wavelengths (negative wave numbers), and Stokes shifting is to longer wavelengths (positive wave numbers). Stokes clearly dominates anti-Stokes at 258 K. (b) Rotational Raman spectrum of O_2 (at 258 K, 310 nm), which contains more lines than for N_2 owing to the effects of electronic spin on angular momentum.

3. Method

The vertical molar abundances (moles/m^2) were determined by integrating the exponential expression $c_0 \exp(-z/H_z)$ with respect to z between the initial and the final altitudes, where c_0 is the concentration of air at the surface in moles/m^3, z is the altitude, and H_z is the scale height and varies with altitude.[9] The upper altitude in this model is 26 km. Above this height the atmospheric pressure is sufficiently low (25 mbar) that the contribution to the total RRS will be negligible.

The temperature and the pressure profile of the U.S. Standard Atmosphere (1976) were used.[10] RRS and thus FI varies with altitude because temperature and pressure are both altitude dependent. Two approaches were used to model this nonhomogeneity. The first approach consisted of dividing the atmosphere into layers with homogeneous temperature. Initially the atmosphere was broken into 1-km sheets. If at a certain altitude, the temperature changed by more than 5%, a new layer began. Otherwise all sheets were grouped together to form a single layer. The result of this breakdown of the atmosphere was a seven-layer model. The temperature for each layer

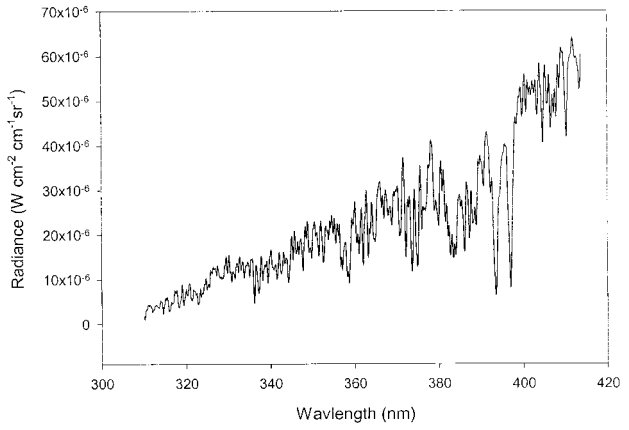

Fig. 2. Radiance of the sky convolved with a triangular slit function with a FWHM of 22 cm^{-1} interpolated to 1 cm^{-1} at a SZA of 61.07°. This is the input spectrum created in MODTRAN3.5 from 310 to 413 nm.

was found by weighting the contribution of each 1-km sheet according to the concentration of air in that sheet. A second approach consisted of using a one-layer atmosphere with the same technique used to find the temperature of the entire layer.

This model uses a sky-radiance spectrum from MODTRAN3.5 as input (see Fig. 2). The effects of elastic-scattering processes (Rayleigh, Mie) and gaseous absorption are thus already included in the input spectrum. Primarily default values were used to create the sky-radiance spectrum in MODTRAN. Some of the important parameter settings used are the U.S. Standard Atmosphere (1976), the radiance mode, multiple scattering by use of Isaac's two-stream approximation, upper and lower altitudes of 26 and 0 km, respectively, and a rural aerosol model (default visibility, 23 km). The solar zenith angle (SZA) specified in MODTRAN3.5 is not particularly important to the FI of lines to the red of 320 nm (where O_3 absorption tails off). This statement can be made partly because elastic scattering does not alter the shape of the spectrum across the wavelength interval of an absorption line; it alters only intensity.

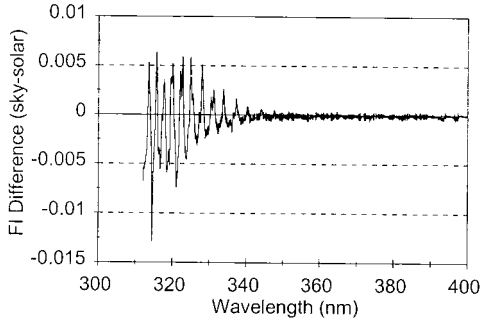

Fig. 3. Effect of ignoring terrestrial absorption on FI values. The sky spectrum and the solar spectrum (both with a resolution of 22 cm^{-1} (a FWHM of a triangular slit function) (at a SZA of 60°) are compared. The difference in FI occurring in the near-UV region is primarily due to Huggins band gas absorption lines (O_3).

Since the Ring effect is also a relative quantity and not an absolute one, only the shape of the spectrum is relevant.[11] As for absorption (the other part of extinction) the intensity of gas-absorption lines, which varies with SZA, is small compared with the large Fraunhofer lines beyond this wavelength. The effect of terrestrial absorption was demonstrated by entering the solar-irradiance spectrum as input instead (see Fig. 3) and comparing the FI. Therefore the correct SZA will be required in the input spectrum only when we are looking at strongly absorbing regions of the spectrum (<320 nm). The main parameters for the solar-irradiance spectrum were the same as for the sky spectrum except that the solar-irradiance mode was selected.

The average of the FI obtained from these two spectra would be an even better approximation of the Ring effect because when the sky spectrum is used, RRS comes after the extinction determined by MODTRAN, whereas when a solar spectrum is used the RRS is modeled before the remaining extinction processes. In reality RRS is occurring simultaneously with these extinction processes, and thus averaging takes the middle of the before (solar) and after (sky) methods and attempts to approximate this simultaneity. Entering the solar spectrum as input was also reasonably close to the value obtained by the averaging method. A difference of at most 7% was found between using a seven-layer model for both methods (sky and solar) and averaging and employing a one-layer method using a single input spectrum (sky or solar).

There are two important points to be made here: (1) resolution and (2) computational time. This difference of 7% was obtained with very-high-resolution spectra (2 cm^{-1}), much higher than the resolution at which most instruments are measuring. Looking at the most recent publications on the Ring effect, we see that the Global Ozone Monitoring Experiment instrument has a spectral resolution of 0.23 nm[2] and the Shuttle Solar Backscatter Ultraviolet Radiometer has a resolution of ~1.1 nm.[5] Chance and Spurr[6] convolved a highly resolved solar spectrum to 0.212 nm in their study. Fish and Jones[12] used a 1-nm zenith-sky spectrometer. At 355 nm, 1.1-nm resolution, for example, is 88 cm^{-1}, far below the resolution used in our test. It will be shown in an upcoming article that the resolution increases linearly by wave number, filling in increases exponentially when plotted versus wavelength. Thus the 7% difference obtained above is an upper estimate of the error associated with this approach. Thus generally the difference between these two methods will be acceptable, particularly in light of the second important point: The computational time required to run the layer model for both input spectra and to average the FI is ~45 min, whereas a one-layer one-input-spectrum model finishes processing the FI in 3–5 min. The computational time of the first method can be optimized significantly, but, in the remainder of this paper, observations, results, and conclusions come from the one-layer sky model.

The frequency-redistributed spectrum is generated

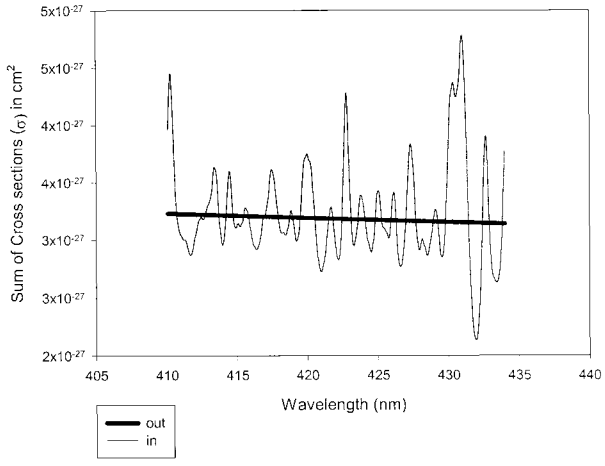

Fig. 4. Sum of cross sections shifting radiance due to RRS (σ_{in} versus σ_{out}), O_2, 410–434 nm. Each point on the thick line represents the sum of the rotational Raman cross sections for the lines shifting light out of that wavelength. The points on the thin line indicate the intensity-weighted cross sections for lines shifting light into a particular wavelength. Note the inverse wavelength dependence for both. The difference between corresponding points on the thick and the thin lines is the cross section inputted into the Beer's law formalism to obtain the frequency-redistributed intensity at a particular wavelength.

by calculating the sky radiance shifted in and out of every 1-cm^{-1} bin. In previous RRS-based Ring effect models (e.g., Ref. 13) only the shifting in has been considered, which is equivalent to the idea of an excess component,[14] but this notion is physically invalid and leads to spectra with no regions of negative FI, contrary to observation.[15]

The radiance shifted into and out of each wave number contains all rotational Raman transitions in which $N < 27$ for nitrogen and $N < 32$ for oxygen. These conditions include Raman lines whose cross section is 3 orders of magnitude weaker than the strongest line. The RRS frequency redistribution is applied one wave number at a time across the entire spectral interval. The cross sections of all the lines shifting light into a particular wave-number bin are weighted by the intensity of the spectrum at the initial wave number. The quantity of σ_{in} is the sum of the cross sections that shift light into a particular wavelength λ from wavelength λ' (see Fig. 4) and can generally be described by

$$\sigma_{in} = 1/I_\lambda \sum_{J,N=0}^{\infty} I_{\lambda'} Q_{N,J\rightarrow N',J';\lambda'}, \quad (7)$$

where I is the intensity (or radiance).

Equation (7) is the sum of the Raman cross sections shifting light into a particular wavelength λ from wavelength λ' (see Fig. 4). The sum of the cross sections shifting light out of the bin with wavelength λ does not require this intensity weighting and is simply

$$\sigma_{out} = \sum_{J,N=0}^{\infty} Q_{N,J\rightarrow N',J';\lambda'}. \quad (8)$$

Subtracting Eq. (8) from Eq. (7) produces a cross-section difference ($\sigma_{out} - \sigma_{in}$) that is then entered into a Beer's law formalism. This method treats RRS as a pseudoabsorption process.[16]

The optical path length (υ_λ) is given simply by $\upsilon_\lambda = (\Delta\sigma_\lambda\, n)$, where n is the number of moles/cm^2. The emergent radiance after RRS is $R_\lambda = I_\lambda \exp(-\upsilon_\lambda)$, where I_λ is the radiance of the sky before RRS. Since $\Delta\sigma$ can be positive or negative, so can υ, leading to positive or negative FI when R_λ is greater or less than I_λ, respectively. The output is the spectrum after frequency redistribution by nitrogen and oxygen through single rotational Raman scattering. Higher-order RRS would be negligible because even two RRS events in Earth's optically thin atmosphere are unlikely as preliminary modeling has shown (<0.04% of all photons will be scattered twice at a SZA of 60°).

Broadening of the Raman lines is relatively insignificant and is omitted as in other studies.[7,12]

The Ring effect is defined as follows:

$$(\mathrm{FI})_\lambda = (I_\lambda - R_\lambda)/I_\lambda, \quad (9)$$

where λ is the wavelength, R_λ is the simulated radiance spectrum with single RRS, I_λ is the simulated radiance spectrum without RRS. It is apparent from Eq. (9) that when the line cores are filled, the FI value will be greater than zero.

At a high SZA the scattering angles for up-looking instruments approach 90°, whereas if the Sun is near the zenith (e.g., SZA is 10°), light entering the instrument will have been scattered at 10°. Because Raman scattered light is slightly polarized (by as much as 8%), there is a greater chance that light will be scattered by RRS at a scattering angle of 10° than at 90°. The RRS phase function, normalized to 4π, is given by

$$P_{\mathrm{RRS}} = (3/40)[13 + \cos^2(\theta)], \quad (10)$$

where θ is the scattering angle.[7] This function can be calculated by substituting the depolarization ratio ρ into the following general phase function, normalized over the solid angle to 4π, which applies to both Rayleigh and RRS:

$$P = 3[(1 + \rho) + (1 - \rho)\cos^2\theta]/(4 + 2\rho). \quad (11)$$

For pure RRS the depolarization ratio is simply 6/7.[6] However, Rayleigh scattering is more polarized than RRS and has the following depolarization ratio:

$$\rho_{\mathrm{Rayleigh}} = 6\varepsilon/(180 + 7\varepsilon), \quad (12)$$

where $\varepsilon = (\gamma/\alpha)^2$ and α (cm^3) is the average polarizability and is given by[17]

$$\alpha = (m^2 - 1)/4\pi N_0, \quad (13)$$

where m is the index of refraction of the medium and N_0 is Loschmidt's number ($=2.686763 \times 10^{19}$ cm^{-3}).

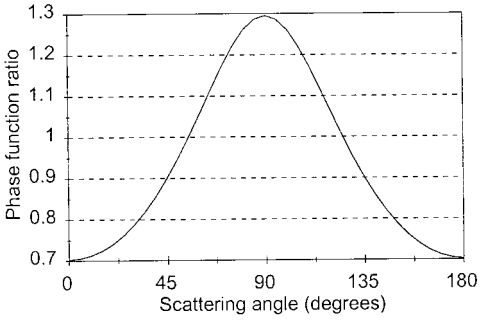

Fig. 5. RRS/Rayleigh phase function ratio versus scattering angle. The weaker dependence of Raman scattering on the cosine of the scattering angle is responsible for the maximum (at 90°) in the ratio of phase functions (RRS/Rayleigh) versus scattering angle.

We calculated the index of refraction for air by using the following equation for air:

$$m_{\text{air}} = 1 + 7.041 \times 10^{-5} + 3.159 \times 10^{6}\ \text{cm}^{-2}/(1.5739 \times 10^{10}\ \text{cm}^{-2} - \nu^2) + 8.4127 \times 10^{4}\ \text{cm}^{-2}/(5.0429 \times 10^{9}\ \text{cm}^{-2} - \nu^2), \quad (14)$$

where ν is the wave number in cm^{-1}. We calculated the polarizability anisotropy for air by weighting the polarizabilities for oxygen and nitrogen according to their relative mixing ratios (1:4).

The ratio of the Raman phase function divided by the Rayleigh phase function is used to predict the diurnal variation of the FI for a known geometry. For zenith-viewing ground-based geometry, one finds that, because this ratio of phase functions increases with SZA, the Ring effect will also increase as a greater fraction of the light received by the instrument is Raman scattered.[11,18] This ratio changes by a factor of 1.84 from 0 to 90° (see Fig. 5), and thus a similar increase in FI can be expected to occur across this SZA range. This direct relationship with SZA has been observed in the majority of ground-based measurements of the Ring effect,[11,12,18] although the opposite has also been frequently observed.[14] The ratio of the phase functions has a very weak dependence on wavelength (a 2% change from 310 to 550 nm), which is ignored in the modeling.

The ratio of the phase functions is unity at cos(SZA) $= 3^{-1/2}$ or SZA = 55°.[17] Thus the columnar abundances must be determined at this SZA. Thus the slant factor for this SZA, calculated for a 26-km-high atmosphere, must be multiplied by the vertical abundances obtained above. Two other factors are important: the diffusivity factor of $3^{1/2}$ that accounts for the multiple scattering when a two-stream approximation is used[17] and the surface-reflection factor. The latter is calculated in the model by 1 + cos(A), where (A) is the albedo and has a value of 0.22, suitable for a grassy surface.[15] Thus multiple scattering and surface reflection are included in this model with regard only to calculation of the optical path length.

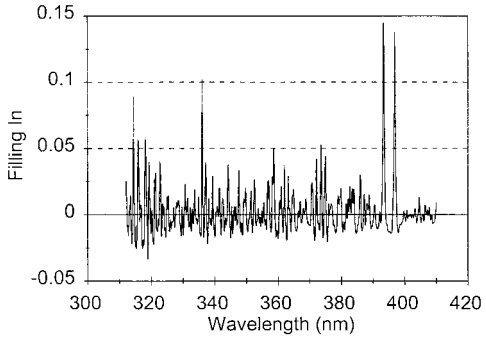

Fig. 6. FI spectrum in the 310–410-nm spectral interval at a resolution of 22 cm^{-1} (FWHM of the triangular slit function); SZA, 30°. Note the large FI for the Ca II K and H lines at approximately 393 and 397 nm, respectively.

4. Observations and Conclusions

The peaks in FI over line centers were found to be symmetrical singlets in all cases even for wide Fraunhofer lines such as the Ca II K and H lines, discounting the hypothesis[15] that asymmetry in the FI could be due to the asymmetry of RRS (Stokes versus anti-Stokes). The appearance of only singlets was in agreement with other studies of the Ca II K and H lines.[5,7,19]

Negative FI values have been observed (see Figs. 6–8). Thus the FI is not produced by an excess component as Noxon and Goody[14] thought. However, the net Ring effect across the entire spectral interval is positive. The FI that is observed in the line centers is light shifted in from the wings of the lines. The corollary of this observation is that the line center will not shift out as much light to the line wings leading to the negative FI that we observe there (Fig. 9). Neglecting the removal of the Ring effect in differential optical absorption spectroscopy (DOAS) leads to an underestimation of the amount of absorber in the gas-absorption line. However, if this gaseous-absorption line is located in the wings of a much larger Fraunhofer line, the gaseous-absorption line could appear deeper than it would without the Ring effect as the negative FI produced by the neighboring Fraunhofer line outweighs the FI of the gas-absorption line. Thus, owing

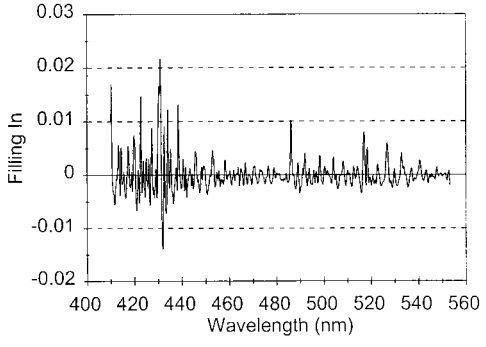

Fig. 7. FI spectrum (410–550 nm) at a resolution of 22 cm^{-1} (FWHM of a triangular slit function); SZA, 30°. No gas-absorption line or Fraunhofer line is filled in above 2.5%.

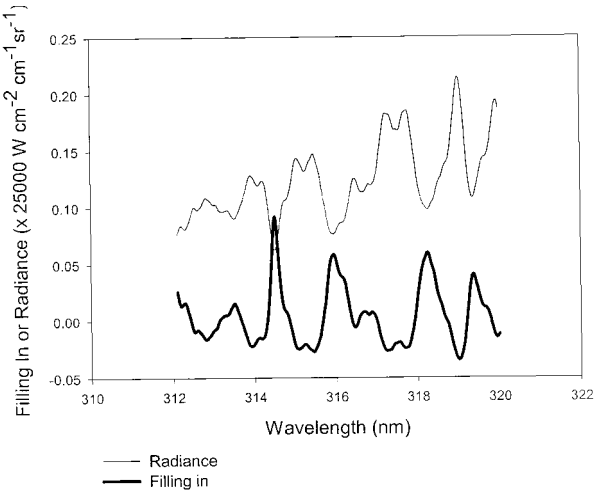

Fig. 8. Radiance spectrum of scattered skylight including RRS and the FI spectrum in the 312–320-nm region at a SZA of 30°. Note the mirror-image pairing of Fraunhofer lines with maxima on the FI spectrum.

to significantly negative FI in the wings and nearby continuum of Fraunhofer lines, DOAS could also be overestimating the concentration of absorbers at these spectral locations if the Ring effect is not taken into account.

Results from this model can be compared with well-described and performed observations or modeling from previous ground-based studies. There must be mention of the SZA used (or it must be calculable), and measurements must fall within the wavelength range used in this study.

Harrison[11] looked at the diurnal variation of the Ring effect over a grassy surface in 3° increments from solar noon (30°) to 90°, using a spectrometer with a slit width of 5 Å. He studied Ca I (422.7 nm), Fe I (433 nm), and Hγ (434.0 nm). Table 1 provides

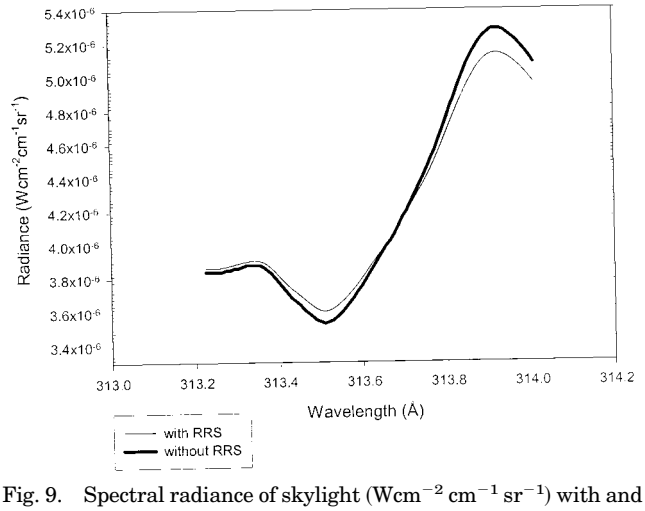

Fig. 9. Spectral radiance of skylight ($Wcm^{-2}\,cm^{-1}\,sr^{-1}$) with and without RRS (thin and thick lines, respectively) for the Ni I line near 313 nm at an SZA of 30°. There is FI in the line core and the opposite effect in the wings of the line (at ~313.9 nm) and in the nearby continuum.

Table 1. FI Comparison (Harrison[a] versus Model) at SZA's of 30° and 90°

Line[b] (nm)	SZA (deg)	FI (%) Harrison[a]	Model (±7%)
422.7 Ca I (1476 mÅ wide)	30	0.9–1.8	1.2
	90	2.2–3.8	2.0
433 Fe I (793 mÅ wide)	30	0.2–1.3	0.6
	90	2.5–3.7	1.0
434.0 Hγ (2855 mÅ wide)	30	0.2–1.5	1.1
	90	2.5–3.7	1.7

[a]Ref. 11.
[b]Line nomenclature and widths were obtained from Lang.[20]

a comparison of his results with output from our model. The resolution of the model is set to 5 Å or 26 cm^{-1} (slit width). The FI is modeled for a SZA of 30° and 90°.

The FI by O_2 and N_2 appears large enough for RRS to be considered the primary mechanism in the Ring effect. However, Harrison's observed diurnal variation is clearly larger. Harrison estimated the diurnal variation to be a factor of 3 between 30° and 90°, but our single-scattering model predicts only a factor of 1.6 (see Fig. 5). Note that in other studies this factor has been observed to be comparable with the one predicted by our model. Joiner *et al.*[5] predicted and observed diurnal variation (30–90°) factors of 1.6, 1.6, and 1.5 in FI for the Mg I line at 285 nm (in the single-scattering regime), near the Ca II K at 393.5 nm and in the blended Fe I line at 358.5 nm (the multiple-scattering regime), respectively.

The measurements by Joiner *et al.*[5] come from the nadir-viewing Solar Backscatter Ultraviolet Radiometer instrument. The scattering angles for the nadir view are the supplementary scattering angles for the zenith view, and, owing to the symmetry of the phase functions about 90° between 0° and 180°, the RRS/Rayleigh phase function ratio is expected to be the same. Thus the diurnal variation is comparable.

The most important points relating to high SZA's is that when the SZA is near 90°, optical path lengths increase sharply with increasing SZA. Thus, at these solar zenith angles, extinction is very high relatively speaking.

Cloud reflection and aerosol scattering are two phenomena not included in the model that attenuate the incoming light beam. As shown by others,[4,7] aerosol (Mie) scattering has the role of diluting the FI since fluorescence is a weak inelastic process and particles are too large to have Raman spectra. In other words, aerosol scattering decreases the inelastically scattered fraction of the beam by increasing the amount of elastic scattering. Establishing the diurnal variation of the Ring effect requires the phase function of these scattering phenomena. Mie scattering is predominantly forward ($\theta = 0°$) (Ref. 17) particularly when the particle size is large, and relatively little scattering occurs beyond $\theta = 90°$. Thus, even after sunset, its contribution to the FI of the zenith-sky spectra relative to Rayleigh scattering

(including Raman) will continue to decrease. Multiple scattering complicates this situation; nevertheless this description could help explain the difference in the observed diurnal variation from ground- and satellite-based measurements. Fish and Jones[12] have also measured the Ring effect from zenith geometry. At high solar zenith angles (higher than 83°), they found that the FI increases dramatically with increasing SZA. Thus, from the available studies observing the diurnal variation of the Ring effect, it appears that the variation in zenith-sky spectra is greater than it is in the nadir view, and we attribute this variation to aerosol scattering. Because aerosols are most concentrated in the lowest 2 km of the atmosphere, they will affect zenith-sky spectra more significantly, causing the diurnal variation of the Ring effect to be greater from the ground. Clouds also play an important yet varying role, depending on their fraction[5] and type.[11]

One conclusion is that the combined effect of multiple scattering, aerosol scattering, and surface reflection on the diurnal variation of the Ring effect can be determined by comparing the phase-function ratio with the observed diurnal variation of the FI values. If, for example, these types of scattering increase the Ring effect, one would expect that the observed diurnal variation factor for FI will exceed the ratio of the phase functions. In other words, to increase the Ring effect, these types of scattering would have to increase the diurnal variation factor to greater than 1.6, because this is the factor predicted by a single Rayleigh-scattering atmosphere including RRS.

We predict that multiple atmospheric scattering for the nadir and the zenith view can only decrease FI at a high SZA (90°), because light of higher-order scattering from angles other than 90° would be present and thus there would be a higher fraction of Rayleigh scattered light. At a low SZA (e.g., 5°) multiple scattering would contribute light that would have a larger Raman-shifted component and thereby increase FI. In the limb view the situation is expected to be the reverse. The authors will study the Ring effect in the limb view with observations from the Optical Spectrograph and InfraRed Imaging System (OSIRIS) (launch date: July 1999).

Observation of the diurnal variation of the Ring effect at twilight would be revealing because the optical path lengths are longer yet; in an aerosol-free atmosphere the inelastic fraction is expected to decrease. Thus over the course of the day, from local noon to sunset, both multiple scattering and the ratio of the phase functions increase, but beyond 90° the ratio of the phase functions decreases whereas multiple scattering continues to increase. Thus, going beyond 90° will help to isolate the precise effect of multiple scattering. Further measurements must be performed to validate previously observed relationships with SZA.

We intend to observe the Ca II K and H lines for which we have obtained extremely high modeled FI values (Ca II K: 25% at a SZA of 90°, 22-cm^{-1} resolution).

Oxygen provided one-third of the FI owing to its spin–spin interaction even though it accounts for only one-fifth of the mixing ratio of the modeled atmosphere. Future modeling should endeavor to determine the result of neglecting the RRS by minor constituents such as polyatomic water.

The wavelength dependence was as expected: FI was magnified at shorter wavelengths. The inverse hypercubic dependence of the Raman cross sections on wavelength (as with Rayleigh scattering) is responsible for this relationship between FI and wavelength. To the red of the Ca II H line (396.85 nm) in this spectral interval, the FI never exceeds 2.5% (the SZA is 30° and the triangular smoothing function FWHM is 22 cm^{-1}). The spectral region beyond 550 nm will be observed in upcoming research to determine the FI of intense Fraunhofer and terrestrial absorption lines in this region. One such line is Hα (656.2808 nm), the third largest Fraunhofer line in the solar spectrum, after the Ca II K and H lines.[20] It is predicted that the Ring effect will be negligible (<1%) with the same SZA and resolution input values.

An important relationship has been observed between spectral resolution and FI as also noted by Burrows *et al.*[2] and Joiner *et al.*[5] This relationship is connected with the wavelength dependence noted above. Because the resolution of the sky spectrum obtained from MODTRAN3.5 is in wave numbers, yet FI is plotted versus wavelength, the FI will be greater and sharper for Fraunhofer lines with decreasing wavelength (see Figs. 6 and 7). The resolution at the UV end (310 nm) of the spectral interval is 194 mÅ, whereas it is 610 mÅ at 555 nm. This resolution helps explain the high FI values obtained in the UV. As the resolution increases, the sky spectrum will have sharper and deeper peaks. Fraunhofer lines in a low-resolution spectrum with only elastic scattering appear filled in (i.e., more shallow and smoothed) compared with the same lines at high resolution. This fact was taken one step further by Kostadinov *et al.*[21] who proposed conveniently adding or removing Ring signatures in sky spectra on the basis of an appropriate slit function.

In conclusion, the strongest FI is observed for well-resolved lines in the UV portion of the spectrum at high SZA's. To maximize FI these lines would be deep so that RRS can fill them substantially and narrow so that the half-width of the line does not exceed the strongest rotational Raman shift (~60 cm^{-1} for N_2 and 49 cm^{-1} for O_2 at 258 K) as it does only for the Ca II K and H lines. As a result these Ca II lines are not as filled in as they would be if they were narrower. However, these lines are the only two Fraunhofer lines filled in beyond 15% (at a SZA of 60°, a slit FWHM of 22 cm^{-1}).

The inclusion of the RRS code into the newest version of MODTRAN would be of both great interest and benefit to the scientific community. This project it is hoped will be undertaken by the authors.

One benefit of building this RRS line-by-line model is that it can simply be inverted to extract the Ring signature (by backward modeling) instead of adding

it to spectra. The authors are in the process of inverting this model and validating its ability to produce spectra that are decontaminated of the Ring effect for application to DOAS.

The authors thank Eldon Puckrin for help with MODTRAN3.5.

References

1. J. R. Grainger and J. Ring, "Anomalous Fraunhofer line profiles," Nature (London) **193,** 762 (1962).
2. J. Burrows, M. Vountas, H. Haug, K. Chance, L. Marquard, K. Muirhead, U. Platt, A. Richter, and V. Rozanov, "Study of the Ring Effect," Technical Report. ESA contract 10996/94/NL/CN (European Space Agency, Noordivijk, The Netherlands, 1996).
3. R. T. Brinkmann, "Rotational Raman Scattering in planetary atmospheres," Astrophys. J. **154,** 1087–1093 (1968).
4. G. W. Kattawar, A. T. Young, and T. J. Humphreys, "Inelastic scattering in planetary atmospheres. I. The Ring effect, without aerosols," Astrophys. J. **243,** 1049–1057 (1981).
5. J. Joiner, P. K. Bhartia, R. P. Cebula, E. Hilsenrath, R. D. McPeters, and H. Park, "Rotational Raman Scattering (Ring effect) in satellite ultraviolet measurements," Appl. Opt. **34,** 4513–4525 (1995).
6. K. V. Chance and R. J. Spurr, "Ring effect studies: Rayleigh scattering, including molecular parameters for rotational Raman scattering, and the Fraunhofer spectrum," Appl. Opt. **36,** 5224–5230 (1997).
7. M. Vountas, V. V. Rozanov, and J. P. Burrows, "Ring effect: impact of rotational Raman scattering on radiative transfer in Earth's atmosphere," J. Quant. Spectrosc. Radiat. Transfer **60,** 943–961 (1998).
8. D. S. Renschler, J. L. Hunt, T. K. McCubbin, Jr., and S. R. Polo, "Triplet structure of the rotational Raman spectrum of oxygen," J. Mol. Spectrosc. **31,** 173–176 (1969).
9. R. P. Wayne, *Chemistry of Atmospheres*, 2nd ed. (Oxford University, Oxford, 1991).
10. A. Berk, L. S. Bernstein, and D. C. Robertson, "MODTRAN: a moderate resolution model for LOWTRAN 7," Tech. Rep. PL-TR-89-0122 (U.S. Air Force Phillips Laboratory, Hanscom Air Force Base, Mass., 1989).
11. A. W. Harrison, "Diurnal variation of the Ring effect," Can. J. Phys. **54,** 1000–1005 (1976).
12. D. J. Fish and R. L. Jones, "Rotational Raman scattering and the ring effect in zenith-sky spectra," Geophys. Res. Lett. **22,** 811–814 (1995).
13. A. W. Harrison, "Computed filling in of Fraunhofer lines 3850–4450 Å," Can. J. Phys. **52,** 2030–2036 (1974).
14. J. F. Noxon and R. Goody, "Noncoherent scattering of skylight," Izv. Acad. Sci. USSR Atmos. Oceanic Phys. **1,** 163–166 (1965).
15. A. W. Harrison and D. J. W. Kendall, "Fraunhofer line filling in (3855–4455 Å)," Can. J. Phys. **52,** 940–944 (1974).
16. S. Solomon, A. L. Schmeltekopf, and R. W. Sanders, "On the interpretation of zenith sky absorption measurements," J. Geophys. Res. **92,** 8311–8319 (1987).
17. K. N. Liou, *An Introduction to Atmospheric Radiation* (Academic, San Diego, Calif., 1980).
18. F. E. Barmore, "The filling-in of Fraunhofer lines in the day sky," J. Atmos. Sci. **32,** 1489–1493 (1975).
19. I. Aben, F. Helderman, D. M. Stam, and P. Stammes, "High-spectral resolution measurements of the atmosphere with the GOME BBM," in *Polarization: Measurement, Analysis, and Remote Sensing*, D. H. Goldstein and R. A. Chipman, eds., Proc. SPIE **3121,** 446–453 (1997).
20. K. R. Lang, *Astrophysical Formulae* (Springer Verlag, New York, 1986).
21. I. Kostadinov, G. Giovanelli, F. Ravegnani, F. Evangelisti, P. Bonasoni, R. Werner, and U. Bonafe, "Polarization and Ring effect influences upon stratospheric DOAS measurements," in *Spectroscopic Atmospheric Monitoring Techniques*, K. Schäfer, ed., Proc. SPIE **3106,** 74–83 (1997).